Rapid Gust Response Simulation of Large Civil Aircraft using Computational Fluid Dynamics

Philipp Bekemeyer
philipp.bekemeyer@liverpool.ac.uk

PhD Student
School of Engineering
University of Liverpool
United Kingdom

Reik Thormann
reik.thormann@liverpool.ac.uk

Research Associate
School of Engineering
University of Liverpool
United Kingdom

Sebastian Timme
sebastian.timme@liverpool.ac.uk

Lecturer
School of Engineering
University of Liverpool
United Kingdom

ABSTRACT

Several critical load cases during the aircraft design process are defined due to atmospheric turbulence. Thus, rapidly performable and highly accurate dynamic response simulations are required to analyse a wide range of parameters. In this paper a method is proposed to predict dynamic loads on an elastically trimmed, large civil aircraft using computational fluid dynamics in conjunction with model reduction. A small sized modal basis is computed by sampling the aerodynamic response at discrete frequencies and applying proper orthogonal decomposition. The linearised Reynolds-averaged Navier-Stokes equations are then projected on the subspace spanned by this basis. The resulting reduced system is solved at an arbitrary number of frequencies to analyse responses to 1-cos gusts very efficiently. Lift coefficients and surface pressure distributions are compared with full order, non-linear, unsteady time-marching simulations to verify the method. Overall, the reduced order model predicts highly accurate global coefficients and surface loads at a fraction of the computational cost.

1.0 Introduction

Dynamic responses to atmospheric turbulence describe several critical load cases during the aircraft design process, demanding highly accurate results at low cost to investigate a large range of parameters. Current industrial practice is based on linear aerodynamics in frequency domain, mostly the doublet lattice method[1]. Thus, examples for this are widespread from isolated wings[2] to full aircraft configurations[3]. While these methods are computationally highly efficient, they can not capture transonic, viscous or thickness effects. In order to improve the accuracy of the predicted loads, correction factors are applied based on either experimental or computational fluid dynamics (CFD) data[4]. However, these corrections are often introduced only at zero frequency and thus deviations at higher frequencies, important for shorter gust lengths, can not be captured accurately.

Despite the overwhelming computational cost, CFD methods alone have been used to investigate gust encounter in the past few years, offering highly accurate results also at non-linear conditions without any additional correction step. Results are available for a wide range of problems from aerofoils to civil aircraft[5,6]. An improvement in efficiency, while maintaining the accuracy of the underlying non-linear CFD model, can be achieved by applying linear frequency-domain methods[7]. The governing equations are linearised around a non-linear steady-state solution assuming small amplitude harmonic motion. Results are widespread from turbomachinery to fixed-wing aircraft including aerofoils and complete airframes, reporting consistently significant cost saving factors, independent of the problem size[8,9,10]. An extension towards gust response simulations has also been published[11,12].

Reduced order modelling is considered a promising approach to further reduce computational cost, while still preserving accuracy[13]. A common model reduction technique is based on proper orthogonal decomposition (POD)[14], first used, in the context of fluid dynamics, to model coherent structures in turbulent flow fields[15]. A small eigenvalue problem, related to snapshots generated by analysing the full system either numerically or experimentally, is solved to obtain POD modes. This approach was soon extended towards frequency-domain sampling data to investigate a rather simple twelve-degrees-of-freedom mass-spring-damper system combined with an incompressible three-dimensional vortex lattice method[16]. Linearised CFD aerodynamics were first considered to analyse the dynamic response of a pitch-plunge aerofoil[17]. More recently, an application for gust responses has been presented for a NACA0012 aerofoil in sub- and transonic flow conditions[11,18], showing excellent agreement at several orders of magnitude reduced computational cost. Combining POD with a linear frequency-domain method not only reduces computational cost further, but, more importantly, an interpolation for frequencies not pre-computed can be avoided. Moreover, a model is obtained which can easily be extended for structural degrees of freedom[11].

This paper presents a reduced order modelling approach for a three-dimensional, industry relevant test case. The full order system behaviour is sampled by computing complex-valued gust responses at several discrete frequencies. Using the standard POD technique, a small eigenvalue problem, correlated to the sampling data, is solved and the number of considered modes is truncated by applying an energy criterion. Obtained modes are discussed to analyse the main region of interest for dynamic gust responses. Once the modal basis is available, the linearised RANS equations are projected onto the POD subspace and rapidly solved for an arbitrary number of frequencies to analyse 1-cos gust responses. Besides lift coefficients also surface pressure distributions are compared between results given by the reduced order model and full-order, unsteady time-marching simulations.

2.0 Numerical Method

The governing equation in semi-discrete vector form is

$$\dot{\mathbf{w}} = \mathbf{R}(\mathbf{w}, \mathbf{v}_\mathrm{g}) \tag{1}$$

where $\mathbf{R}$ is the non-linear residual corresponding to the fluid unknowns $\mathbf{w}$, while $\mathbf{v}_\mathrm{g}$ denotes external disturbances due to gusts. The difference between an equilibrium solution $\mathbf{w}_0$ and the state-space vector $\mathbf{w}$ is introduced as

$$\Delta\mathbf{w} = \mathbf{w} - \mathbf{w}_0 \tag{2}$$

and accordingly for external disturbances. A first order Taylor expansion is used to express the change in residual around the equilibrium point

$$\Delta\dot{\mathbf{w}} = \mathbf{R}(\mathbf{w}_0, \mathbf{v}_{\mathrm{g}0}) + \frac{\partial \mathbf{R}}{\partial \mathbf{w}}\Delta\mathbf{w} + \frac{\partial \mathbf{R}}{\partial \mathbf{v}_\mathrm{g}}\Delta\mathbf{v}_\mathrm{g} \tag{3}$$

where $\frac{\partial \mathbf{R}}{\partial \mathbf{w}}$ describes the Jacobian matrix A and $\mathbf{R}(\mathbf{w}_0, \mathbf{v}_{g0})$ is by definition zero.

Assuming harmonic motions for the disturbance vector $\Delta\mathbf{w}$ and external excitation vector $\Delta\mathbf{v}_\mathrm{g}$, the system is transferred into frequency domain. Thus, Eq. (3) becomes

$$(A - i\omega I)\,\hat{\mathbf{w}} = -\frac{\partial \mathbf{R}}{\partial \mathbf{v}_\mathrm{g}}\hat{\mathbf{v}}_\mathrm{g} \tag{4}$$

with $\hat{\mathbf{w}}$ and $\hat{\mathbf{v}}_\mathrm{g}$ denoting complex-valued Fourier coefficients. The right-hand side is constructed by using a matrix-free finite-difference evaluation for the matrix-vector product $\frac{\partial \mathbf{R}}{\partial \mathbf{v}_\mathrm{g}}\hat{\mathbf{v}}_\mathrm{g}$ while applying an analytical description for the vector $\hat{\mathbf{v}}_\mathrm{g}$. Further detail can be found in previous publications about the frequency-domain gust response method[11,12].

2.1 Proper Orthogonal Decomposition

The full order model is sampled at K discrete frequencies by solving Eq. (4) while adjusting the right-hand side term accordingly. Obtained solutions $\hat{\mathbf{w}}$ are stored as columns in the snapshot matrix S as

$$S = \left[\hat{\mathbf{w}}^1, \hat{\mathbf{w}}^2, \ldots, \hat{\mathbf{w}}^K\right] \tag{5}$$

The columns of the POD basis Φ are linear combination of the snapshot matrix entries as

$$\varphi_k = S\,\boldsymbol{\nu}_k \tag{6}$$

Unit length of basis vectors φ is ensured by scaling $\boldsymbol{\nu}_k$. The best possible approximation in Eq. (6) is then obtained by solving the corresponding eigenvalue problem of dimension K

$$S^H S\,\boldsymbol{\nu}_k = \lambda_k \boldsymbol{\nu}_k \tag{7}$$

Since $S^H S$ is positive definite and symmetric all eigenvalues λ_k are real and positive. The relative information content contributed to the system by a certain mode, also often referred to as energy, is given by

$$r_k = \lambda_k \left(\sum_{i=0}^{K} \lambda_i\right)^{-1} \tag{8}$$

and can be used to decrease the number of modes further by only considering those with a high relative information content. The corresponding reduced order model (ROM) is constructed by expressing the state-space vector $\hat{\mathbf{w}}$ as

$$\hat{\mathbf{w}} = \Phi\hat{\mathbf{z}} \tag{9}$$

The small sized reduced system is obtained through a Galerkin projection on Eq. (4)

$$\left(\Phi^H A\Phi - i\omega I\right)\hat{\mathbf{z}} = -\Phi^H \frac{\partial \mathbf{R}}{\partial \mathbf{v}_\mathrm{g}}\hat{\mathbf{v}}_\mathrm{g} \tag{10}$$

Solving the ROM, represented by Eq. (10), at an arbitrary number of frequencies and then reconstructing full order solutions is an efficient way to investigate dynamic gust responses. Since an analytical derivation of the matrix $\frac{\partial \mathbf{R}}{\partial \mathbf{v}_\mathrm{g}}$ is currently under development, all right-hand sides for the ROM in the current work are sampled, projected and stored explicitly while forming the model.

2.2 Computational Fluid Dynamics Method

Results are produced by the DLR-TAU code[19] solving the RANS equations in conjunction with the Spalart-Allmaras turbulence model[20]. The field velocity approach which adds an artificial mesh velocity based on the defined excitation shape is used to incorporate gusts[21]. Inviscid fluxes are discretised by applying a central scheme with scalar artificial dissipation of Jameson, Schmidt and Turkel[22] while the Green-Gauss theorem is used to compute gradients, necessary for viscous and source terms. Steady-state solutions are obtained by utilising local time-stepping and the backward Euler method with lower-upper Symmetric-Gauss-Seidel iterations[23]. Convergence is further accelerated using a 2v multigrid cycle.

All unsteady simulations are performed using dual time-stepping together with the second order backward differentiation formula. Unsteady, time-dependent gust response simulations are produced with a time-step size of 0.00178 s and a fixed number of time steps of 1024, based on previous numerical experiments. The linear frequency-domain formulation used for snapshot generation follows a first-discretise-then-linearise, matrix-forming approach with an analytical, hand-differentiated Jacobian matrix. Linear systems are then solved using a generalised conjugate residual solver with deflated restarting[24]. For preconditioning a block incomplete lower-upper factorisation of the Jacobian matrix with zero level of fill-in is applied[25]. In total 100 Krylov vectors, 20 of which are part in the deflated restarting process, are applied to solve the system. A decrease of seven orders of magnitude for the density residual is used as convergence criterion. Since the reduced order model is built assuming that the snapshots form a subspace of the eigenspace of the Jacobian matrix, the convergence criterion needs to be chosen more strictly compared to a direct frequency-domain gust analysis[12].

3.0 Results

A large civil aircraft with a wingspan of approximately 60 m is investigated to demonstrate the maturity of the method for a test case of industrial interest. The mesh shown in Fig. 1(a) consists of nearly 8 million points, of which 130,000 are on the surface. An elastic trimming procedure based on Broyden's method[26], balancing lift and weight while ensuring zero pitching moment, is used to obtain a steady-state solution at a representative freestream

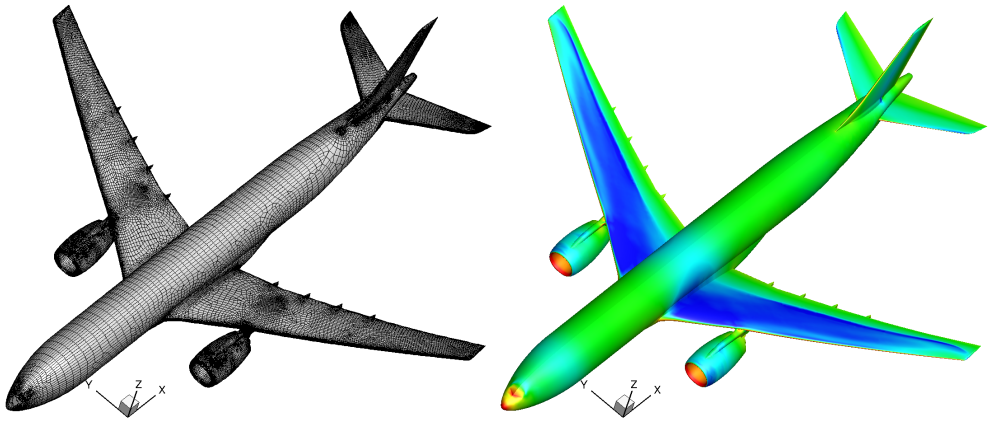

(a) Surface point distribution (b) Steady surface pressure distribution

Figure 1: Surface mesh and steady-state surface pressure coefficient for civil aircraft

Mach number and altitude. In total 94 structural modes are included and an artificial trimming mode adjusting the elevator deflection is applied. During the trimming process, the elevator deflection and the angle of attack are iteratively adjusted until the desired coefficients are reached. Within each iteration step the mesh is deformed according to computed surface loads which are projected onto the structural modes. Finally the magnitude of the density residual is driven to converge seven orders of magnitude. The steady surface pressure distribution, shown in Fig. 1(b), contains a strong shock along the wingspan at roughly 70% chord length. A decrease of sectional lift towards the wing tip is caused by wing bending together with torsion. Since the elevator is deflected during the trimming process, a strong suction area around the leading edge is observed while no shock formation is present.

The system response is sampled at 15 linearly spaced reduced frequencies between 0 and 0.5. Different sampling strategies, including an exponential distribution, have not been tested yet and might prove beneficial since for aerofoil responses an improvement was observed[11]. Further, the inclusion of the complex conjugate of the snapshots while forming the reduced order basis is not necessary since positive frequencies are sufficient to capture the system behaviour. The relative information content of all possible 15 POD modes is displayed in Fig. 2(a). With nearly 75%, the most of the energy is contained in the first mode while the information content of all other modes decays nearly exponentially. The final mode has an energy content which is approximately six orders of magnitude below the first mode.

The pressure field for the first POD mode is shown globally, around the main wing and around the tail in Figs. 2(b)-2(d), respectively. Several slices are displayed to visualise the three-dimensional structure of the POD mode also inside the flow field. The affected areas of the first POD mode are mainly the wing and the elevator while no pressure fluctuations are present along the fuselage. On the upper wing surface, the governing flow features, namely the shock formation and the suction area around the leading edge, are clearly visible and describe the area of highest variations. Inside the field high values are concentrated close to the surface, and in particular around these two areas, while further away from the surface the flow field is unaffected. Comparing inboard and outboard sections of the wing, it is found that

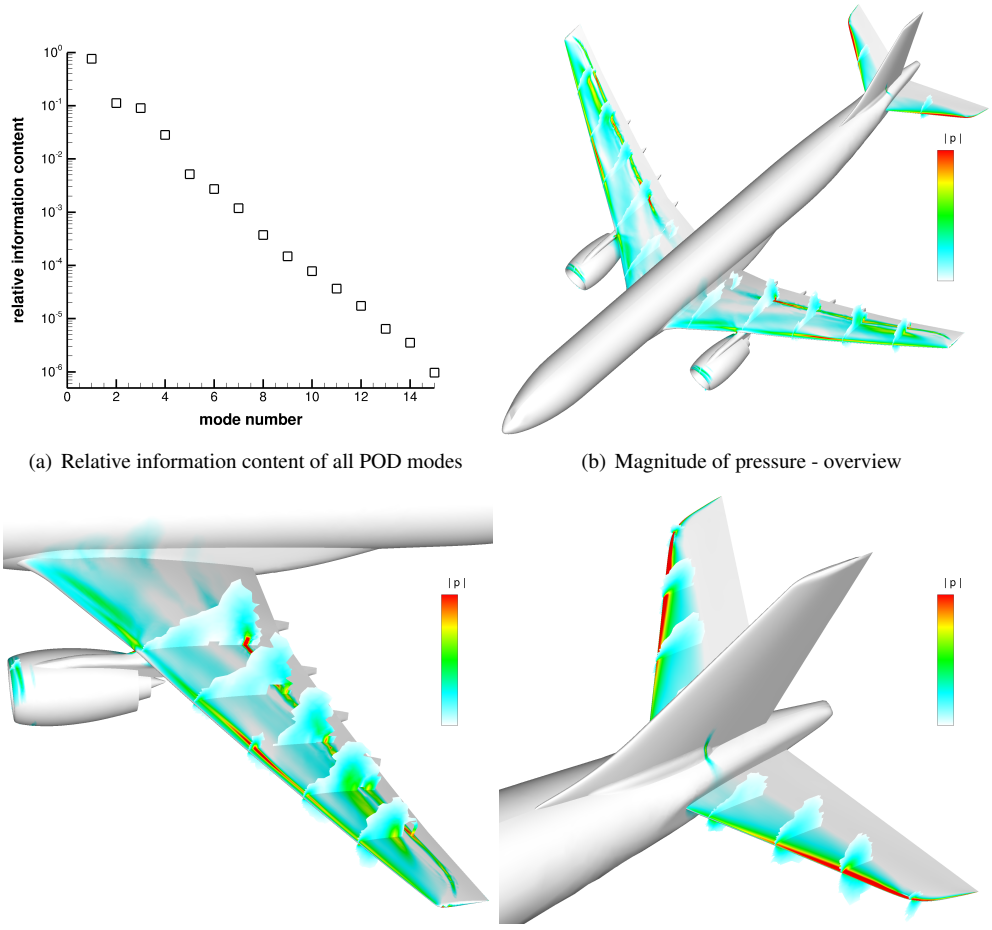

(a) Relative information content of all POD modes

(b) Magnitude of pressure - overview

(c) Magnitude of pressure around wing

(d) Magnitude of pressure around tail

Figure 2: Relative information content of all POD modes and magnitude of pressure for first POD mode

the POD mode contains dominant features in the outboard region supporting the fact that gust loads define the outer wing structure. With no shock formation present on the tail, the elevator exhibits pressure deviations only around the suction line at the leading edge.

The influence of energy retained inside the ROM is investigated using a 1-cos gust with gust length $L_g = 116$ m and an amplitude of 0.001% of the freestream velocity to ensure a dynamically linear response of the full order time-marching solution. Since the reduced linear system is small, the spacing and number of considered frequencies for solving Eq. (10) is of minor concern. However, it should be ensured that only frequencies inside the sampling range are used since extrapolation is causing a significant reduction in accuracy for POD based models. Time histories of the lift coefficient for the full order reference solution and three reduced order models, which differ in the retained relative information content, are presented in Fig. 3(a). If 99.999% of the relative information content is included, resulting in

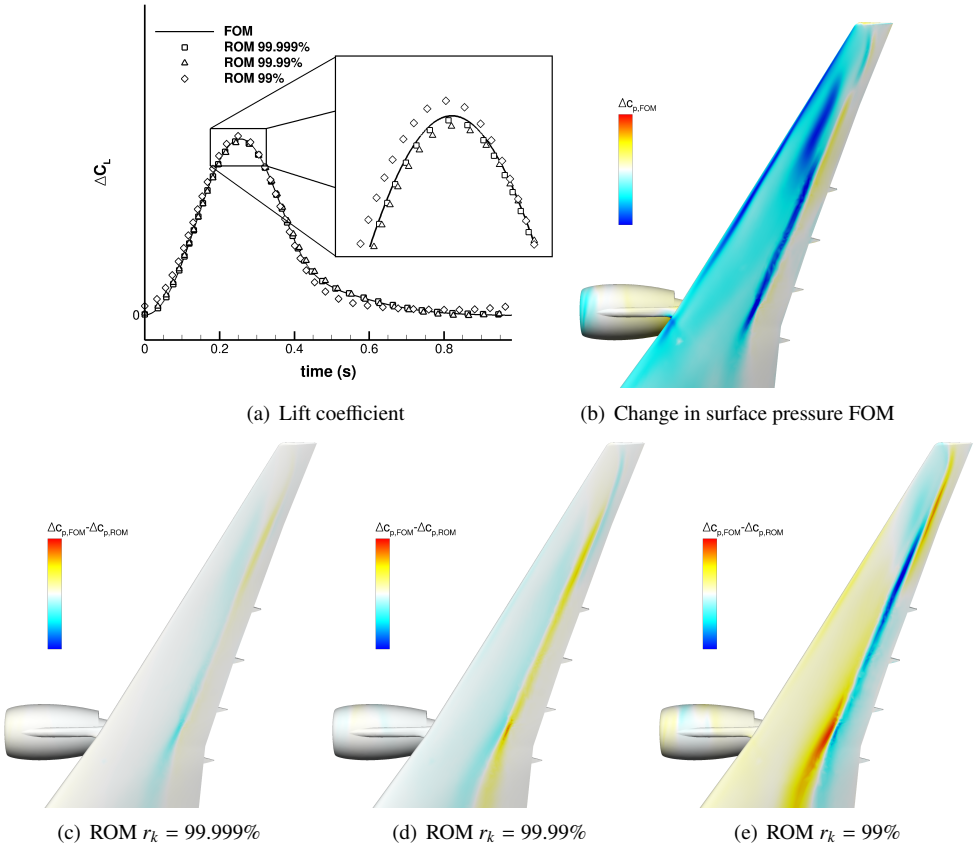

(a) Lift coefficient (b) Change in surface pressure FOM

(c) ROM r_k = 99.999% (d) ROM r_k = 99.99% (e) ROM r_k = 99%

Figure 3: Investigation of modes retained in POD ROM using a 1-cos gust with L_g = 116 m for time history of lift coefficient and change in surface pressure at $\Delta C_{L,max}$

12 out of 15 possible modes, the time-domain signal is rebuilt accurately. When the energy is decreased to 99.99%, reducing the number of modes to 7, also the peak value decreases while the global shape, including the lift decay, is preserved. Finally, retaining 99%, the overall tendency is still correct but besides the peak value also the lift decay is no longer represented. Furthermore, results start to deviate from the steady solution since only 4 modes are retained. Surface pressure distributions on the starboard wing are compared between the full order model (FOM) reference solution (Fig. 3(b)) and the three different ROMs, shown in Figs. 3(c)-3(e). With decreasing mode number, the surface pressure around the shock position becomes more indistinct while slight deviations are visible throughout the wing. In addition, if 99% of the energy is retained, differences are clearly visible close to the wing tip, resulting in an additional outer wing shock which is not present in the FOM solution. For all remaining results, 12 modes are retained to identify occurring loads as accurately as possible. Thus, a huge reduction is achieved compared to the nearly 50 million degrees of freedom of the full system. Moreover, a even stronger reduction in size is possible when sacrificing accuracy.

Task	Cost
Time-domain simulation	1
Reduced order model build-up (total cost)	0.345
a) Calculating snapshots and POD basis	0.320
b) Pre-sampling right-hand side data	0.025
Solving ROM for a single 1-cos gust	10^{-6}
Post-processing	
a) Rebuilding global coefficients	10^{-8}
b) Rebuilding surfaces loads	10^{-6}

Table 1: Comparison of computational cost

Computational cost for building the reduced order model, as well as for solving it, is displayed in Tab. 1. Since both, the ROM and the unsteady time-marching approach, require a steady-state solution, computational cost of the elastic trimming process is excluded. All values are non-dimensionalised by the computational cost necessary to compute a full-order, time-domain reference solution. The most expensive part during the ROM generation is the frequency-domain sampling process with 0.345. However, sampling all snapshots in frequency domain already offers a cost saving factor of about 3 compared to one full-order, unsteady time-marching solution. While the current model also needs to evaluate right-hand sides during the model construction, such cost, even though low at 0.025, can be avoided when an analytical description of the right-hand side matrix in Eq. (10) is available, causing the efficiency of the generation process to increase further. Obtaining a 1-cos response using the ROM is approximately six orders of magnitude faster then solving the full order model while global coefficients, such as lift and pitching moment, are available at essentially no additional cost. Moreover, reconstructing surface pressure distributions is computationally as expensive as solving the reduced model. Shear forces and moments, essential during the aircraft design process, are produced together with the pressure distributions and thus come at no additional computational cost.

Once the reduced order model is available, several 1-cos gusts can be analysed at negligible computational cost. Dynamic responses for the coefficient of lift for three different representative gust lengths, namely L_g = 58 m, 116 m and 174 m, are visualised in Fig. 4(a). Excellent agreement between the reduced model and the full order reference solutions is obtained for all gust lengths. Only minor differences occur around maximum lift as already discussed above. When looking at the pitching moment coefficient in Fig. 4(b) again good agreement is found. However, besides the slight deviations around the peak values also minor oscillations arise during the moment decay for the shortest gust length. Creating sampling data also at higher frequencies by applying an exponential instead of a linear snapshot distribution might increase the accuracy of the ROM also for shorter gust length.

Finally the ROM is used to investigate a dynamic response to a realistic 1-cos gust as defined by the European Aviation Safety Agency in CS 25.341[27]. The gust length is chosen as L_g = 116 m and the amplitude is nearly 7% of the freestream velocity. The change in lift coefficient over time is shown in Fig. 5(a). While for the global shape good agreement is observed, minor differences in the maximum lift value as well as in the lift decay are visible. These discrepancies are caused by a dynamically non-linear response near the maximum lift coefficient during the time-marching simulation. The ROM, however, is constructed by a

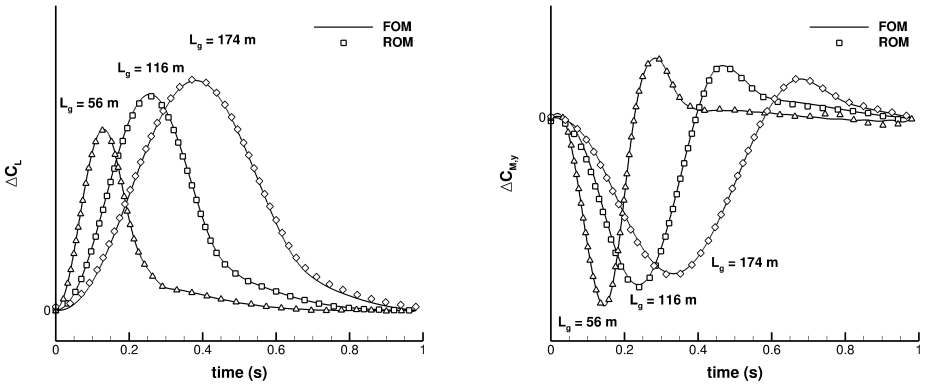

(a) Lift coefficient (b) Pitching moment coefficient

Figure 4: Time histories of lift and pitching moment coefficient for 1-cos gusts with L_g = 58 m, 116 m and 174 m

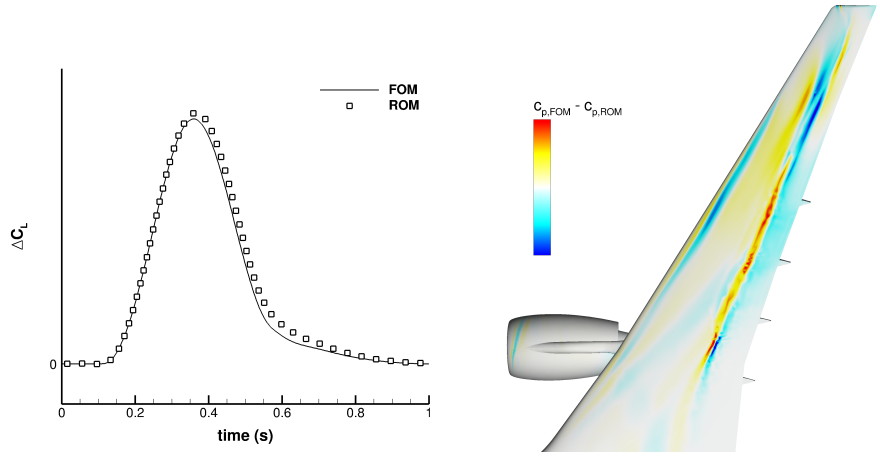

(a) Lift coefficient (b) Surface-pressure difference

Figure 5: Time history of lift coefficient and surface-pressure difference at peak load for 1-cos gust with L_g = 116 m

time-linearised RANS method and thus assumes a dynamically linear response, resulting in a slight overprediction of the maximum lift coefficient. Nevertheless, the ROM conservatively predicts loads at various orders of magnitude reduced computational cost. The absolute surface pressure difference at maximum lift coefficient is displayed in Fig. 5(b) to estimate the discrepancies when comparing both simulation techniques further. Since a non-linear shock motion and a non-linear amplitude decrease occur during the time-domain analysis, the highest error arises around the shock location. In addition, some minor discrepancies are present around the leading edge, caused by the same amplitude mechanism.

4.0 Conclusions

This paper outlines a method to compute aerodynamic responses to gust encounter at several orders of magnitude reduced computational cost while preserving the accuracy of the underlying computational fluid dynamics solver. The governing Reynolds-averaged Navier-Stokes equations are linearised and transferred into frequency domain before projecting them on a small sized modal basis. Proper orthogonal decomposition is applied for model reduction, based on sampling data generated at a few discrete frequencies using a linear frequency-domain solver. Following the projection, an arbitrary number of 1-cos gust responses can be obtained at negligible computational cost on a local desktop machine.

The presented test case is an elastically trimmed passenger aircraft at transonic flight conditions. The full order model is sampled at 15 equally spaced reduced frequencies between 0 and 0.5 in order to construct a proper orthogonal decomposition based reduced order model. The relative information content of all possible modes is discussed and the first mode is analysed. Afterwards, a reduced order model is created by retaining 12 modes, equivalent to 99.999% of the relative information content. Compared to the full order model with nearly 50 million degrees of freedom a massive reduction in size is achieved. While accuracy is preserved when analysing various 1-cos gust responses using the applied strict energy criterion, reducing the retained relative information content could offer a more practical and applied solution since even stronger reductions are possible. Finally, the model is used to investigate a gust as defined by international certification regulations, showing good and conservative load predictions at several orders of magnitude reduced computational cost.

An analytical derivation of the gust influence term on the right-hand side is currently in progress to improve the efficiency of the model reduction approach further. Also, the introduction of a combined modal basis using the presented proper orthogonal decomposition basis and Schur traced structural eigenmodes is planned to analyse coupled fluid-structure responses. Finally, the transformation of the model into time domain is considered to be able to incorporate a control system for gust load alleviation.

Acknowledgements

The research leading to these results was co-funded by Innovate UK, the UK's innovation agency, as part of the Enhanced Fidelity Transonic Wing project.

REFERENCES

1. Albano, E. and Rodden, W. P., "A doublet lattice method for calculating lift distribution on oscillating surfaces in subsonic flow," *AIAA Journal*, Vol. 2, No. 7, 1969, pp. 279–285.
2. Giesing, J. P., Rodden, W. P., and Stahl, B., "Sears Function and Lifting Surface Theory for Harmonic Gust Fields," *Journal of Aircraft*, Vol. 7, 1970, pp. 252–255.
3. Kier, T., "Comparison of Unsteady Aerodynamic Modelling Methodologies with Respect to Flight Loads Analysis," *AIAA Atmospheric Flight Mechanics Conference and Exhibit*, 2005, AIAA 2005-6027.
4. Dimitrov, D. and Thormann, R., "DLM-Correction Methods for Aerodynamic Gust

Response Prediction," *International Forum on Aeroelasticity and Structural Dynamics (IFASD)*, 2013, IFASD 2013-24C.

5. Raveh, D. E., "CFD-Based Models of Aerodynamic Gust Response," *Journal of Aircraft*, Vol. 44, No. 3, 2007, pp. 888–897.
6. Reimer, L., Ritter, M., Heinrich, R., and Krüger, W., "CFD-based Gust Load Analysis for a Free-flying Flexible Passenger Aircraft in Comparison to a DLM-based Approach," *22nd AIAA Computational Fluid Dynamics Conference*, 2015, AIAA 2015-2455.
7. Thormann, R., Nitzsche, J., and Widhalm, M., "Time-linearized Simulation of Unsteady Transonic Flows with Shock-Induced Separation," *European Congress on Computational Methods in Applied Sciences and Engineering*, 2012, ECCOMAS 2012.
8. Clark, W. S. and Hall, K. C., "A Time-Linearized Analysis of Stall Flutter," *Journal of Turbomachinery*, Vol. 122, No. 3, 2000, pp. 467–476.
9. Weishäupl, C. and Laschka, B., "Small Disturbance Euler Simulations for Delta Wing Unsteady Flows due to Harmonic Oscillations," *Journal of Aircraft*, Vol. 41, No. 4, 2004, pp. 782–789.
10. Thormann, R. and Widhalm, M., "Linear-Frequency-Domain Predictions of Dynamic-Response Data for Viscous Transonic Flows," *AIAA Journal*, Vol. 51, No. 11, 2013, pp. 2540–2557.
11. Bekemeyer, P. and Timme, S., "Reduced Order Gust Response Simulation using Computational Fluid Dynamics," *57th AIAA/ASCE/AHS/ASC Structures, Structural Dynamics, and Materials Conference*, 2016, AIAA 2016-1485.
12. Bekemeyer, P., Thormann, R., and Timme, S., "Linearised Frequency Domain Gust Response Analysis of Large Civil Aircraft," *European Congress on Computational Methods in Applied Sciences and Engineering (ECCOMAS)*, 2016, ECCOMAS 2016-5316.
13. Lucia, D. J., Beran, P. S., and Silva, W. A., "Reduced-order modeling: new approaches for computational physics," *Progress in Aerospace Sciences*, Vol. 40, No. 1-2, 2004, pp. 51–117.
14. Dowell, E. H. and Hall, K. C., "Reduced Order Models in Unsteady Aerodynamic Models, Aeroelasticity and Molecular Dynamics," *ICAS - 26th Congress of International Council of the Aeronautical Sciences*, 2008, ICAS 2008-0.1.
15. Lumley, J. L., "The Structures of Inhomogeneous Turbulent Flow," *Atmospheric Turbulence and Radio Wave Propagation*, 1967, pp. 166–178.
16. Kim, T., "Frequency-Domain Karhunen-Loève Method and Its Application to Linear Dynamic Systems," *AIAA Journal*, Vol. 36, No. 11, 1998, pp. 2117–2123.
17. Hall, K. C., Thomas, J. P., and Dowell, E. H., "Proper Orthogonal Decomposition Technique for Transonic Unsteady Aerodynamic Flows," *AIAA Journal*, Vol. 38, No. 10, 2000, pp. 1853–1862.
18. Thormann, R., Bekemeyer, P., and Timme, S., "Reduced Order Modelling of Gust Analysis Using Computational Fluid Dynamics," *European Congress on Computational Methods in Applied Sciences and Engineering (ECCOMAS)*, 2016, ECCOMAS 2016-5441.
19. Schwamborn, D., Gerhold, T., and Heinrich, R., "The DLR TAU-Code: Recent Applications in Research and Industry," *European Conference on Computational Fluid Dy-*

namics, 2006, ECCOMAS CFD 2006.

20. Spalart, P. R. and Allmaras, S. R., "A One-Equation Turbulence Model for Aerodynamic Flows," *Recherche Aerospatiale*, Vol. 1, 1994, pp. 5–21.
21. Parameswaran, V. and Baeder, J. D., "Indicial aerodynamics in compressible flow-direct computational fluid dynamic calculations," *Journal of Aircraft*, Vol. 34, No. 1, 1997, pp. 131–133.
22. Jameson, A., Schmidt, W., and Turkel, E., "Numerical Solutions of the Euler Equations by Finite Volume Methods Using Runge-Kutta Time-Stepping Schemes," *AIAA Journal*, 1981, pp. 1981–1259.
23. Dwight, R., "An Implicit LU-SGS Scheme for Finite-Volume Discretizations of the Navier-Stokes Equations on Hybrid Grids," *DLR-FB-2005-05*, 2006.
24. Xu, S., Timme, S., and Badcock, K. J., "Krylov Subspace Recycling for Linearised Aerodynamics Analysis using DLR-TAU," *International Forum on Aeroelasticity and Structural Dynamics (IFASD)*, 2015, IFASD-2015-186.
25. Saad, Y., *Iterative Methods for Sparse Linear Systems*, Society for Industrial and Applied Mathematics, Philadelphia, PA, 2nd ed., 2003.
26. Broyden, C. G., "A class of methods for solving nonlinear simultaneous equations," *Mathematics of Computation (American Mathematical Society)*, Vol. 19, 1965, pp. 577–593.
27. European Aviation Safety Agency, "Certification Specifications for Large Aeroplanes (CS-25)," 2015.